Chemical Engineering & Processing: Process Intensification 172 (2022) 108787

Contents lists available at ScienceDirect

Chemical Engineering and Processing - Process Intensification

journal homepage: www.elsevier.com/locate/cep

Different cases study on the heating surface layout of a new 600 MWe coal-fired power plant coupled with CaO-based carbon capture system based on heat exchanger network

Zhixin Li, Qinhui Wang *, Mengxiang Fang, Zhongyang Luo

State Key Laboratory of Clean Energy Utilization, Zhejiang University, Hangzhou, Zhejiang 310027, China

ARTICLE INFO

Keywords:
Cao-based carbon capture system
Heat exchanger network
Heat exchange area
Coal-fired power plant

ABSTRACT

This work provides a practical engineering design on the new 600 MWe coal-fired power plant coupled with CaO-based carbon capture system. Three heating surface layout cases are proposed in order to realize the high temperature heat source of the new power plant to heat the feed water into the superheated steam (24.2 MPa, 566 °C). In addition, pipeline calculation and economic analysis for three cases are carried out. The results show that the heat exchange area of three cases increases, respectively by around 33.5%, 47.3% and 53.7% as comparing to the benchmark 600 MWe coal-fired power plant under the carbon capture efficiency of the coupled system is around 90%. In the pipeline design, the flue gas resistance of case 1 through heat exchange pipeline is about 0.74 MPa. The economic analysis shows that case 1 has a slight advantage as comparing to cases 2 and 3. The research provides a good direction for future research direction of the coal-fired power plant coupled with CaO-based carbon capture system.

1. Introduction

Nowadays, the increase of living demand leads to an increasing trend of energy consumption. Excessive utilization of fossil fuels will lead to excessive gas emissions, included CO_2 and other greenhouse gasses, which will cause a series of environmental problems [1,2]. Carbon capture technology has always been an important method to reduce carbon dioxide emission and attracted extensive attention from numerous scholars [3–5], which mainly contains pre-combustion capture, oxy-fuel combustion and post-combustion capture [4,5].

Calcium-based carbon capture is regarded as a very promising post-combustion carbon capture technology, which was first proposed by Professor Shimizu et al. in 1999 [6]. The process of this technology contains CO_2 capture in carbonator and regeneration of CaO-based adsorbents in calciner. CaO particles reacted with CO_2 in carbonator at around 650 °C to produce $CaCO_3$ particles. After the carbonation reaction, calcium carbonate particles are calcined in calciner at 900 °C to regenerate CaO adsorbents [7,8], plenty of fresh calcium carbonate is needed to make up for deactivated CaO-based adsorbent during calcination. High-concentration carbon dioxide at the outlet of calciner is condensed and compressed for industrial application. The process of CaO-based carbon capture technology is shown in Fig. 1.

The flue gas from outlet of carbonator and calciner in the CaO-based carbon capture system are high temperature heat sources. If the flue gas is directly discharged into the atmosphere, which will cause a large amount of energy waste, so it is necessary to make reasonable use of waste heat. The research focuses on the coupling between CaO-based carbon capture system and other energy power systems, including the integration of coal-fired power plant and solar power plant with CaO-based carbon capture system [9–11]. Zhang et al. [12] proposed two optimization schemes of adding a set of 300 MWe steam configuration and performing parallel distribution of feed water based on the coal-fired power plant coupled calcium-based carbon capture system. Zhou et al. [13] evaluated the concept of a low-temperature CO_2 capture device based on a 1000 MWe thermal power plant. Hanak et al. [14] studied a 580 MWe supercritical coal-fired power plant integrated calcium circulation system and showed that the integrated system efficiency decreased by about 8.6%. Duan et al. [15] proposed the coupled carbon capture system into coal-fired power plants and analyzed the influence of adding a re-carbonation system on the coupled system. Ortiz et al. [16] calculated the energy loss after the coupling of a coal-fired power plant and carbon capture system. Romano [17] studied the coupled double-fluidized bed CaO-based carbon capture system, amine carbon capture system and oxy-enriched combustion system in coal-fired power plant. Spinelli et al. [18] employed a cement plant with

* Corresponding author.
E-mail address: qhwang@zju.edu.cn (Q. Wang).

https://doi.org/10.1016/j.cep.2022.108787
Received 17 September 2021; Received in revised form 6 December 2021; Accepted 5 January 2022
Available online 10 January 2022

Nomenclature

AQ	the air quantity
FW	feed water
WIT	inlet feed water temperature
WOT	outlet feed water temperature
HT	heat transfer
LT	logarithmic mean temperature
AT	air velocity
FG	the flue gas
FIT	inlet flue gas temperature
FOT	outlet flue gas temperature
HC	heat transfer coefficient
HA	heat exchange area
EM	economizer
WCW	water wall
LS	low temperature superheater
MS	medium temperature superheater
HS	high temperature superheater
LR	low temperature reheater
HR	high temperature reheater
LR1	low temperature reheater1
LR2	low temperature reheater2
LR3	low temperature reheater3
HR1	high temperature reheater1
HR2	high temperature reheater2

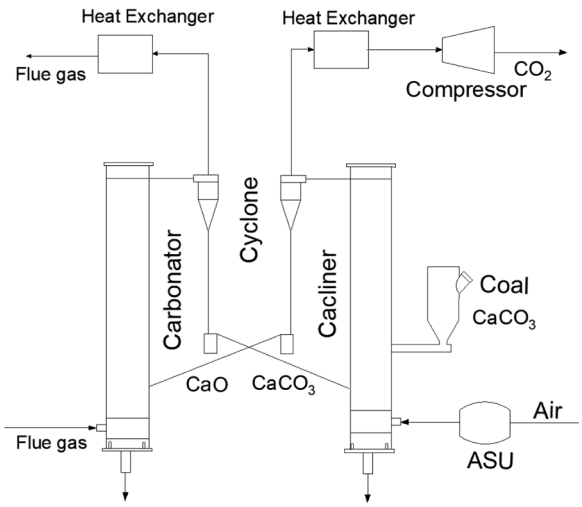

Fig. 1. Process of calcium-based carbon capture system.

a CaO-based carbon capture system and verified the feasibility of the system in practical application. Lee et al. [19] explored the efficiency of natural gas industry combined with carbon capture system. Berstad et al. [20] simulated six schemes of natural gas combustion (NGCC) combined with calcium-based carbon capture system, and the results showed that the carbon capture efficiency of integrated system reached more than 90%.

Heat exchanger network has been a research hotspot in recent years, which has been used in many research fields based on the relationship between temperature gradient and heat transfer gradient of different cold and hot sources [21–23]. Ziyatdinov et al. [24] proposed a new iterative sequence algorithm for heat exchanger network optimization and applied the method to several heat integral problems. Kayange et al. [25] studied the optimization problem of heat exchanger network based on the diverging unstructured mode. Xia et al. [26] analyzed the comprehensive problem of heat exchanger network based on entransy theory and found that the entransy transfer efficiency was 92.29%. Lai et al. [27] explored the structure, parameterization process and utility changes of step diagram to existing heat exchanger network, and applied the proposed method to an existing crude oil refinery. It is undoubtedly beneficial to the optimization and practical application of the coupling system if the heat between cold and hot sources of multiple coupling systems can be systematically calculated based on heat exchanger network. Meanwhile, there are few studies on the research of heat exchanger network involving coal-fired power plant coupled with CaO-based carbon capture system, so the detailed discussion of this work is of certain research significance.

In this work, the reasonable matching and utilization of high temperature heat source in the new 600 MWe coal-fired power plant coupled with CaO-based carbon capture system is studied based on the heat exchanger network. Three heating surface layout cases are put forward. The pipeline design and economic analysis of the coupled system are performed.

2. Preparation process

2.1. Heat exchanger network of the new 600 MWe coal-fired power plant coupled with CaO-based carbon capture system

The new 600 MWe coal-fired power plant coupled with CaO-based carbon capture system contains coal-fired boiler, CaO-based carbon capture, steam turbine, air separation and other units. The whole system contains three high-temperature heat sources, which are flue gas from coal-fired boiler, carbonator and calciner. It could be defined the flue gas at the outlet of the carbonator, the calciner, the coal-fired boiler in the new power plant as F-1, F-2, F-3, and defined the feed water and high temperature steam of different temperature ranges as S-1, S-2, S-3 and S-4, respectively. Table 1 shows the exchange heat and temperature of different cold and hot sources. The energy distributions of different cold and heat sources are shown in Fig. 2, it can be seen that the span of high and low temperature of heat source covers almost all the temperature gradient of cold flow. Table 1 shows that the heat of coal-fired boiler unit is around 800 MW, accounting for 69.7% of the total high-temperature heat. It can be clearly seen in Fig. 2 that the straight line of the coal-fired boiler spans almost all temperatures, so the heat source of coal-fired boiler can be selected to heat the high-parameter steam. On the whole, we can see that the heat source of coal-fired boiler in the new power plant is more suitable for heating feed water or steam that needs more heat, and the heat source of carbon capture unit is more suitable for heating the steam that needs less heat.

2.2. Calculation procedure of the new 600 MWe coal-fired power plant coupled with CaO-based carbon capture system

In order to better understand the design results of the new power plant, we explain the calculation process of the new power plant as following:

(1) Determining the inlet and outlet temperature of feed water or high-temperature steam of different heat exchange equipment in the new power plant.
(2) Based on the heat exchanger network, the steam or feed water of different heat exchange equipment in the new power plant corresponding to the three heat sources of flue gas are determined.

Table 1
Specific parameters of different heat sources of new 600 MWe coal-fired power plant.

		Temperature before heat exchange/ °C	Temperature after heat exchange/ °C	Heat transfer/MW
F-1	Flue gas at the outlet of carbonator	645	140	218.9
F-2	Flue gas at the outlet of calciner	900	140	129.2
F-3	Hot source of coal-fired boiler	1533	140	800
S-1	Cold flow 1	250	295	133
S-2	Cold flow 2	290	388	399.8
S-3	Cold flow 3	380	566	313.46
S-4	Cold flow 4	323	566	217.68

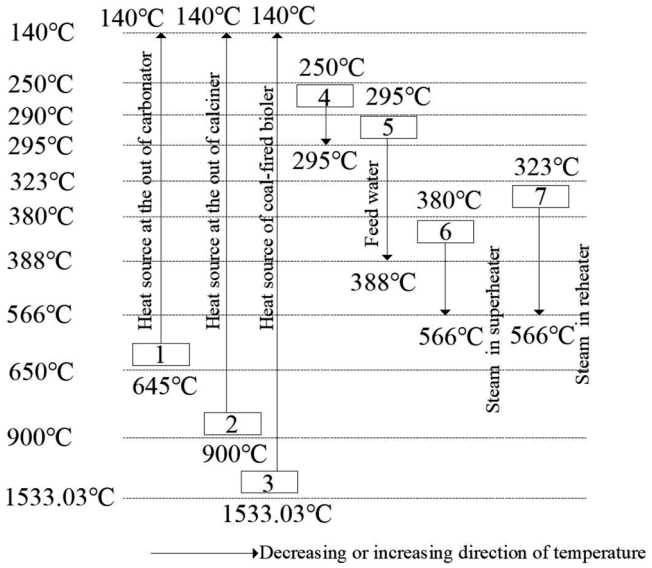

Fig. 2. Energy system diagram of heat exchanger network for the new 600 MWe coal-fired power plant.

(3) Determining the inlet and outlet temperature of the high-temperature flue gas passing through the heat exchange equipment of the new power plant.
(4) Determining the exchange area of the heat exchange equipment.
(5) Comparison of heat exchange area of heat exchange equipment in the new power plant under different cases.

The logarithmic mean temperature and heat exchange area can be expressed as follows:

$$\Delta T = \frac{(T_1 - T_2) - (T_3 - T_4)}{In\left(\frac{T_1 - T_2}{T_3 - T_4}\right)} \quad (1)$$

Where ΔT is logarithmic mean temperature, T_1 *and* T_2, T_3 *and* T_4 are temperature of hot and cold flow at the outlet of exchanger, temperature of hot and cold flow at the inlet of exchanger.

$$A = \frac{Q}{F\Delta T} \quad (2)$$

Where A is heat exchange area, Q is the exchange of heat, F is heat transfer coefficient, ΔT is logarithmic mean temperature.

3. Cases of heat source utilization in the new 600 MWe coal-fired power plant coupled with CaO-based carbon capture system

The simulation results of a benchmark 600 MWe coal-fired power plant are shown in Table 2, the design principles are determined by reference [12]. Fig. 3 shows the heat load ratio of all heat exchange surface in the benchmark 600 MWe coal-fired power plant. The feed water is about 1612 t/h, and the heat exchange area reaches 27,964 m^2. The heat transfer coefficient (F) of all heat exchange surfaces is referred from the literature [28], which is chosen around 80 W/m^2K for superheater, reheater, economizer and around 180 W/m^2K for water wall.

The flue gas contains 13.3% CO_2 out of coal-fired boiler for the new 600 MWe coal-fired power plant passes through the carbonator is

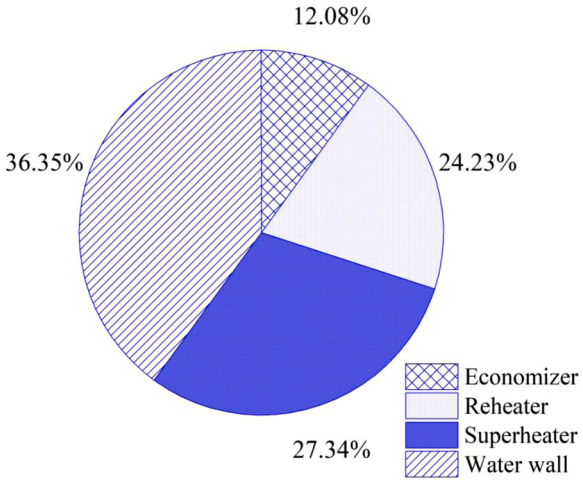

Fig. 3. Different heat load ratio of heating surface in the benchmark 600 MWe coal-fired power plant.

Table 2
Design results of benchmark 600 MWe coal-fired power plant.

	EM	WCW	LS	MS	HS	LR	HR
FW/t/h	1612	1612	1612	1612	1612	1556	1556
WIT / °C	250	290	375	400	500	322.6	430
WOT/ °C	295	380	425	525	566	450	566
HT/MW	133	399	64	153	83	101	165
LT	250	1012	383	579	616	289	3951
AT /m/s	–	–	10.5	10.6	10.6	10.5	10.7
FG/Nm^3/ h	1776,015	1776,015	1776,015	1776,015	1776,015	1776,015	1776,015
FIT / °C	600	1516	815	1112	1187	751	972
FOT/ °C	452	1187	751	972	1112	600	815
HC/W/m^2K	80	180	70	70	80	70	80
HA /m^2	6629	3286	2376	3771	1692	5003	5207

1264,192 Nm^3/h, the carbon capture efficiency in carbonator is set at 90%. Three hot sources are used to heat the feed water of the new power plant to produce supercritical high temperature steam. Main principle is that high-temperature flue gas at the outlet of CaO-based carbon capture and coal-fired boiler units are employed to heat the steam in different heat exchange devices, including water wall, reheater, superheater and economizer, etc.

3.1. Case 1: heating conjointly full feed water with three hot sources

In case 1, the hot sources of coal-fired boiler and CaO-based carbon capture units in the new 600 MWe coal-fired power plant heat all the feed water. Fig. 4 shows the process of new 600 MWe coal power plant coupled CaO-based carbon capture system. The flue gas of coal-fired boiler heats the feed water through water wall, further heats the steam in the high temperature superheater and medium temperature superheater, and then heats the steam in the high temperature reheater and low temperature reheater. The flue gas at the outlet of carbonator heats the high temperature steam in low temperature superheater, low temperature reheater and economizer. The flue gas of calciner heats high temperature steam in the high temperature and low temperature reheater. The flue gas from three heat sources is employed to heat air by air preheater in the end. It can be seen from Table 3 that the feed water is 1626.86 t/h, the heat exchange area reaches 37,333 m^2. Compared with the benchmark 600 MWe coal-fired power plant, the heat exchange area increases by 9369 m^2, which is about 33.5%. The heat transfer coefficient of all heat exchange surfaces is consistent with benchmark coal-fired power plant. Fig. 5 shows the heat load ratio of all heat exchange surface. The increase in heat exchange area is mainly concentrated on the heating surface passed by two heat sources of CaO-based carbon capture unit, which in low temperature superheater increases by 2373 m^2, in high temperature and low temperature reheater increases by 1787 m^2 and 4186 m^2, respectively. The heat exchange area of other device increases slightly in different degrees.

The increase of heat exchange area can be explained as the heat source of the benchmark coal-fired power plant is equivalent to the sum of three hot sources in new 600 MWe coal-fired power plant. Therefore, compared with the 600 MWe benchmark power plant, the temperature of heat source will decrease faster with anyone of the three hot sources in the new 600 MWe coal-fired power plant when the same heat is heated for feed water. Decreasing temperature quickly will get smaller logarithmic mean temperature (ΔT), which means the heat exchange area will increase ultimately. As shown in Tables 2 and 3, the logarithmic mean temperature (ΔT) in the low-temperature superheater, low-temperature reheater and low-temperature superheater in the new 600 MWe power plant decreases significantly as comparing to the benchmark 600 MWe coal-fired power plant, which results in greatly increase in the heat exchange area. On the whole, the heat exchange area of low temperature superheater, low temperature reheater and high temperature reheater increases by 2373 m^2, 4186 m^2 and 1787 m^2, respectively. In addition, the steam in three parts heat exchange equipment is mainly heated by the heat source of the carbon capture unit.

3.2. Case 2: heating part of feed water with hot source of coal-fired boiler and part of feed water with hot source of carbon capture unit

As shown in Fig. 6, feed water is distributed in parallel for generating high temperature steam in case 2. The two-part feed water is heated by the high temperature heat source of coal-fired boiler and CaO-based carbon capture unit in the new power plant. After passing through water wall, the flue gas of coal-fired boiler heats the steam of high temperature superheater, medium temperature superheater and low temperature superheater, respectively, and continues to heat the steam in the high-temperature reheater and low-temperature reheater. The flue gas of carbonator heats the steam in the medium-temperature superheater, further heats the steam in the low-temperature superheater and the low-temperature reheater. The flue gas of calciner heats the steam in the high-temperature superheater and high-temperature reheater. At last, three hot sources heat the air together through air preheater. The heat load ratio of all heat exchange surface is shown in Fig. 7. The results in Table 4 show that the feed water of coal-fired boiler and carbon capture units are 1162 t/h and 465 t/h, respectively. The heat exchange area of new 600 MWe coal-fired power plant is 41,188 m^2, which is about 47.3% more than that of benchmark 600 MWe coal power plant.

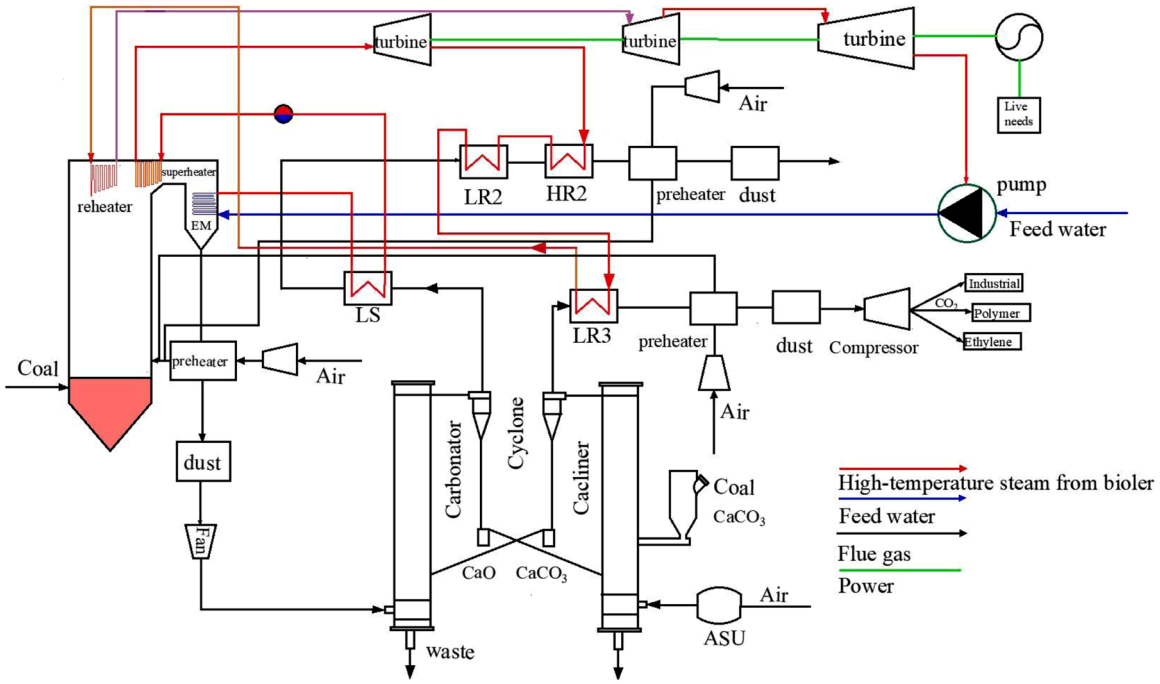

Fig. 4. Process of the new 600 MWe coal-fired power plant. Heating conjointly full feed water with three hot sources in the new 600 MWe coal-fired power plant.

Table 3
Design results of the new 600 MWe coal-fired power plant under case 1.

	EM	WCW	LS	MS	HS	LR1	LR2	LR3	HR1	HR2
FW/t/h	1627	1627	1627	1627	1627	1560	1560	1560	1560	1560
WIT/ °C	250	290	375	400	500	322.6	400	420	430	515
WOT/ °C	295	380	425	525	566	400	420	450	515	566
HT/MW	132	400	64	161	88	61	15	25	71	45
LT	142	951	194	386	472	182	111	96	208	205
AT /m/s	–	–	11	11.1	11.1	10.6	10.8	10.7	11	11
FG/Nm^3/ h	1109,863	1264,192	1109,863	1264,192	1264,192	1264,192	1109,863	281,803	1262,918	281,803
FIT/ °C	500	1533	645	946	1064	609	542	625	753	900
FOT/ °C	360	1064	542	753	946	478	500	466	609	629
HC/ W/m^2K	80	180	70	75	80	70	75	75	80	80
HA/m^2	6165	2335	4749	5577	2324	4208	1687	3294	4267	2727

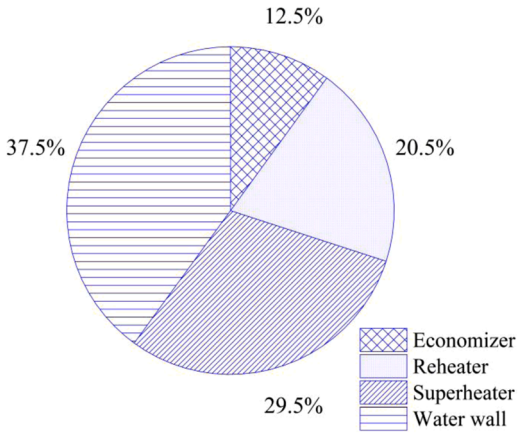

Fig. 5. Case 1: Different heat load ratio of heating surface in the new 600 MWe coal-fired power plant.

Heat exchange area of case 2 increases by about 3855 m^2 as comparing to the case 1, it can be explained that the heat in the carbon capture unit is little as comparing to coal-fired boiler unit, so the logarithmic mean temperature is small in the process of heat transfer. By comparing Tables 3 and 4, it can be seen that the logarithmic mean temperature (ΔT) in the high-temperature superheater, medium-

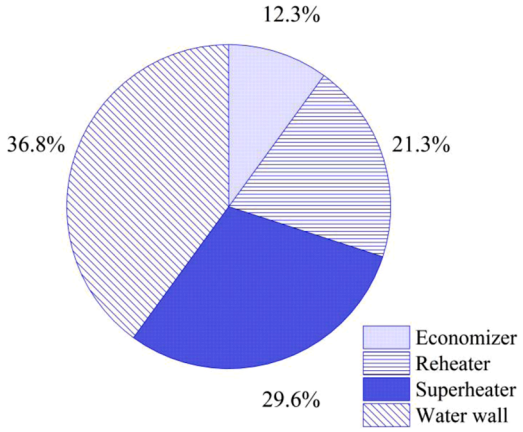

Fig. 7. Case 2: Different heat load ratio of heating surface in new 600 MWe coal-fired power plant.

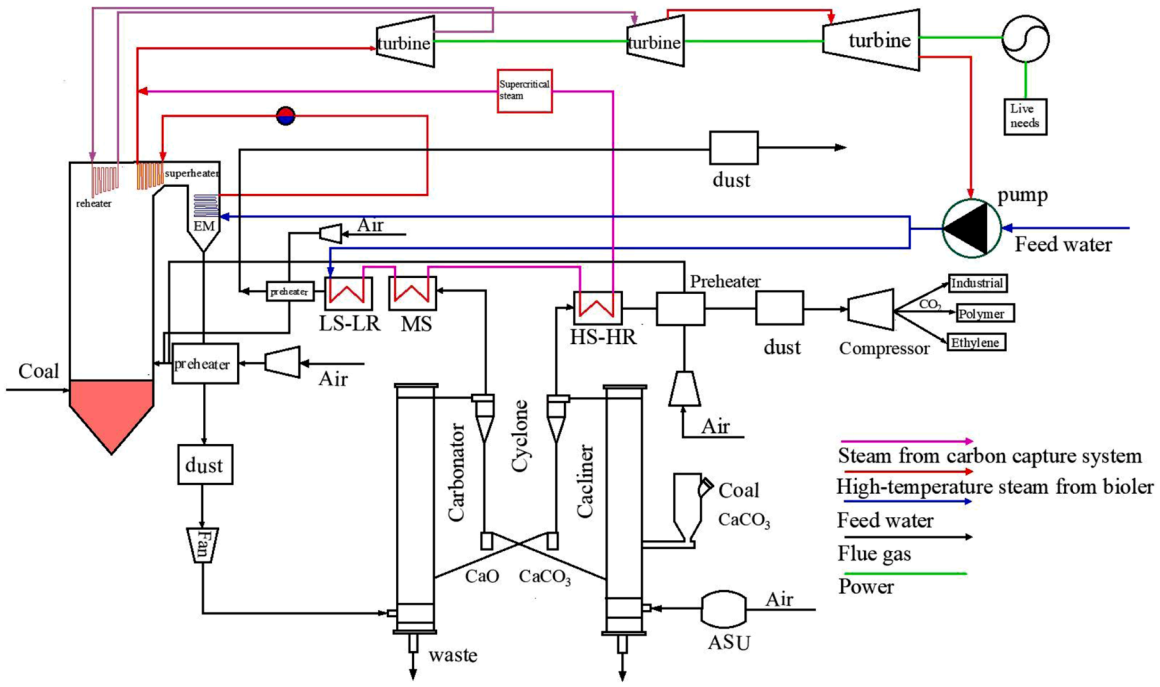

Fig. 6. Process of the new 600 MWe coal-fired power plant. Heating part of feed water with hot source of coal-fired boiler unit and part of feed water with hot source of carbon capture unit in the new 600 MWe coal-fired power plant.

Table 4
Design results of the new 600 MWe coal-fired power plant under case 2.

	EM	WCW	LS	MS		HS	LR	HR	EM	LS	MS	HS	LR	HR
	Coal fired boiler unit								Carbon capture system unit					
FW/t/h	1162	1162	1162	1162	1162	1162	1150	1150	465	465	465	465	460	460
WIT / °C	250	290	375	400	500	500	322.6	430	260	375	400	500	322.6	430
WOT / °C	295	380	425	525	566	566	450	566	295	425	525	566	450	566
HT/MW	85	400	47	85	86	86	73	91	40	22	40	42.	28	40
LT	197	951	281	434	476	476	207	279	179	151	144	279	114	141
AT/m/s	–	–	10.8	10.6	11	11	10.2	10.8	–	10.8	10.6	11	10.2	10.8
FG/Nm^3/h	1264,192	1264,192	1264,192	1264,192	1264,192	1264,192	1264,192	1264,192	281,803	1109,863	1109,863	281,803	1109,863	281,803
FIT / °C	539	1533	714.7	954	1064	1064	647	840	550	572	645	900	530	730
FOT/ °C	406	1064	647	840	954	954	539	715	380	530	572	730	478	550
HC/W/m^{2}K	80	180	70	75	80	80	75	80	80	70	72	80	70	80
HA /m^2	5400	2335	2412	2607	2259	2259	4399	4063	2792	2093	3871	1897	3510	3550

temperature superheater and high-temperature reheater in case 2 decreases significantly as comparing to that in case 1. The heat exchange area of the three parts device increases by 1832 m^2, 901 m^2 and 619 m^2, respectively. However, case 2 is more convenient for application of the new 600 MWe coal-fired power plant, which can be reasonably arranged on the position where heat exchange device is located.

In terms of heat load ratio of different heat exchangers, the results of two cases are similar to that of the benchmark 600 MWe coal-fired power plant. From the perspective of practical application, the new 600 MWe coal-fired power plant coupled with CaO-based carbon capture system has higher requirement for the complicated layout of heat exchangers, so it has not been widely applied in industrial applications so far [29–31].

3.3. Case 3: heating part of feed water with hot source of coal-fired boiler and part of feed water with hot source of carbon capture unit (the hot source of carbon capture unit is used in different ways)

As shown in Fig. 8, the hot source of the CaO-based carbon capture unit is allocated to heat the steam in different method as comparing to case 2. The flue gas of calciner heats the steam in the high temperature reheater, and then heats the steam in medium temperature superheater and low temperature superheater, respectively. The flue gas of the carbonator heats the steam in high temperature superheater, and then heats the steam in low temperature reheater. Finally, two hot sources of carbon capture unit are employed to heat the air. The heat load ratio of all heat exchange surface of case 3 is consistent with case 2.

Table 5 indicates that the heat exchange area of case 3 is around 42,979 m^2, including water wall, superheater, reheater, economizer and other units. Compared with benchmark 600 MWe coal-fired power plant, the heat exchange area increases approximately 15,015 m^2, which increases around 53.7%. The heat exchange area needed in case 3 is 1791 m^2 more than case 2. As shown in Table 4 and Table 5, the increasing area of high temperature superheater in case 3 is obvious as comparing to case 2, which increases by about 5313 m^2. It could be seen in the high temperature superheater steam is mainly heated by flue gas from carbonator in case 3, and by flue gas from calciner in case 2, which can save the heat exchange area. It is understood that the design concept of case 2 has a slight advantage.

4. Pipeline calculations of the new 600 MWe coal-fired power plant coupled with Cao-based carbon capture system

The pipeline design for the new 600 MWe coal-fired power plant is arranged in case 1. It is not necessary to elaborate on other cases based on the pipeline calculation of different cases are generally the same. In case 1, there is a great difference in area of different heat exchange equipment, so different calculation methods should be adopted to design different heat exchange equipment. A great amount of flue gas will bring about obvious flue gas resistance, the steam velocity is generally selected around 11 m/s [32]. The flue gas resistance in the pipeline is calculated by the following formula:

$$h_f = \lambda * \frac{l}{d} * \frac{v^2}{2g} \tag{3}$$

Where h_f is the flue gas resistance, L is pipe length, D is pipe diameter, V is the flow rate, λ is the drag coefficient along pipeline, g is the acceleration of gravity.

Table 6 shows the pipeline design of new 600 MWe coal-fired power plant coupled with CaO-based carbon capture system. All the pipes used in the design process have an outer diameter of 42, 40 and 36 mm, respectively. In addition, the greater steam velocity is, the higher heat transfer rate will be. However, the larger steam velocity will lead to greater resistance. The results show that the flue gas resistance of reheater and superheater reaches 0.67 MPa and 0.07 MPa, respectively.

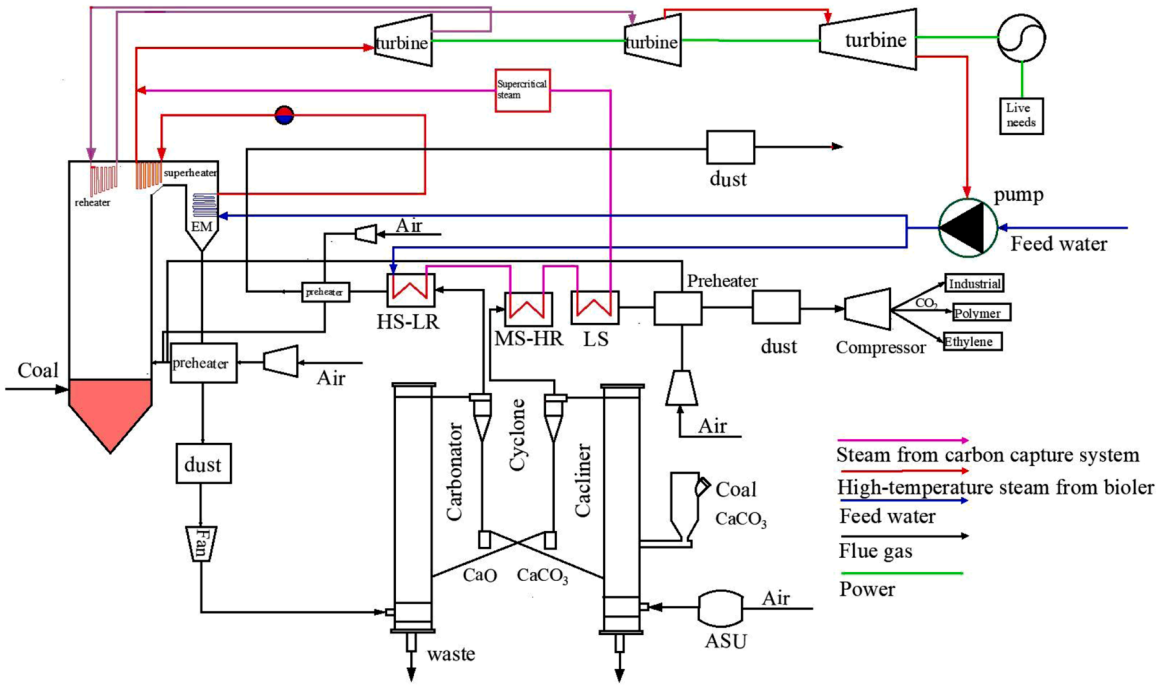

Fig. 8. Process of the new 600 MWe coal-fired power plant. Heating part of feed water with hot source of coal-fired boiler unit and part of feed water with hot source of carbon capture unit (the hot source of carbon capture unit is used in different ways).

Therefore, the flue gas resistance is mainly concentrated in the reheater, which mainly because the reheater has longer pipeline. The resistance along all pipelines is about 0.74 MPa.

5. Economic analysis of three cases

We carry out the economic analysis on three cases. The heat exchange equipment in the new 600 MWe coal-fired power plant constructed from the materials, which are consistent with the materials used in reference [33]. Table 7 shows the types and prices of materials used for different heat exchange equipment, which based on market research in China. Fig. 9 shows the price of water wall, superheater, reheater and economizer of three cases. Cases 2 and 3 have a significant increase in the price of superheater and reheater, and a slight increase in the price of economizer as comparing to case 1. It suggests that the three high-temperature heat sources in the new 600 MWe coal-fired power plant are mainly used to heat the steam in superheater and reheater for cases 2 and 3. As shown in Fig.10, the increase of pipe thickness will lead to the increase of equipment price of the new 600 MWe coal-fired power plant. With fixed the heat exchange area, the smaller the thickness is, the smaller the material volume is, and the lower equipment cost will be. When the outer diameter of the pipeline is constant, the smaller pipeline thickness means the less pipeline length required, which could reduce the resistance along the pipeline. However, the larger pipe diameter, the smaller steam flow rate will be, which may not reach the minimum steam flow rate for the new 600 MWe coal-fired power plant.

6. Contrastive analysis and thermodynamic analysis of three cases

As shown in Table 8, the heat exchange area of case 1 is less than cases 2 and 3. The heat exchange area of case 2 and case 3 increases by 10.3% and 15.1% as comparing to case 1. The heat exchange area of cases 1, 2 and 3 is 37,333, 41,188, 42,979 m^2, respectively. The heat exchange area of all cases is larger than that of the benchmark coal-fired power plant, which caused by total heat energy is divided into multiple reservoirs. On the while, the case 1 has a slight advantage compared with other cases.

For the proposed cases in this work, thermodynamic analysis is needed to be performed. The thermodynamic analysis results of the new 600 MWe coal-fired power plant have been revealed in the literature [34]. It can be seen that compared with the benchmark 600 MWe coal-fired power plant, the system efficiency of the new power plant shows a decreasing trend, which decreases about 8.3%. The main reason for the decrease of system efficiency is the energy consumption of oxygen production in the process of oxygen-rich combustion and carbon dioxide compression. At the same time, the coal consumption and feed water of the new power plants under the three cases are basically the same, so the boiler efficiency and system efficiency of the new power plant under the three cases are consistent. Main difference of the three cases is the heating surface layout of the new power plant, which will further lead to the change of the heat exchange area for the new power plant. Therefore, the research angle of this work is feasible.

7. Conclusion

During the work, heating surface layout in a new 600 MWe coal-fired power plant coupled with CaO-based carbon capture system is explored based on the heat exchanger network. Three different design cases for the new 600 MWe coal power plant coupled with CaO-based carbon capture system is completed. The main results are showed as following:

(1) In case 1, the high temperature of the new power plant heat sources is used to heat all the feed water. In cases 2 and 3, the feed water is distributed in parallel, and the feed water is heated independently by the high temperature heat sources of coal-fired boiler and CaO-based carbon capture units. The three cases have their own characteristics, which provide reference for the industrial application of new coal-fired power plant coupled CaO-based carbon capture system.
(2) Heat exchange area of the new 600 MWe coal power plant coupled with carbon capture system in the case 1 increases by 33.5% as comparing to that of the benchmark 600 MWe coal

Table 5
Design results of the new 600 MWe coal-fired power plant under case 3.

	EM	WCW	LS	MS	HS	LR	HR	EM	LS	MS	HS	LR	HR
	Coal fired boiler unit							**Carbon capture system unit**					
FW/t/h	1162	1162.2	1162.2	1162.2	1162.2	1150	1150	465	465	465	465	460	460
WIT/ °C	250	290	375	400	500	322.6	430	260	375	400	500	322.6	430
WOT/ °C	295	380	425	525	566	450	566	295	425	525	566	450	566
HT/MW	85	400	47	85	86	73	91	40	22	40	42	28	40
LT	197	951	281	434	476	207	279	179	128	195	73	152	321
AT/m/s	–	–	10.8	10.6	11	10.2	10.8	–	10.8	10.8	10.8	10.3	10.2
FG/Nm^3/h	1264,192	1264,192	1264,192	1264,192	1264,192	1264,192	1264,192	1109,863	281,803	281,803	1109,863	1109,863	281,803
FIT / °C	539	1533	715	954	1064	647	840	568	578	739	645	568	900
FOT/ °C	406	1064	647	840	954	539	715	380	478	578	568	515	739
HC/ W/m^{2}K	80	180	70	75	80	75	80	80	70	72	80	70	80
HA/m^2	5400	2335	2412	2607	2259	4399	4063	2792	2467	2857	7210	2623	1555

Table 6
Pipeline calculation of the new 600 MWe coal-fired power plant under case 1.

	Pipe diameter/ mm	Pipe length/ m	Pipe number	Pipe pitch/ m	Flow rate/ m/s	Resistance/ Pa
HR1	42	92.9	385	6.2	11	16,431
HR2	42	58.6	390	5.86	11	10,104
LR1	36	164.2	255	8.21	10.6	571,143
LR2	36	46.4	360	4.7	10.8	59,866
LR3	36	72.06	455	7.21	10.7	14,850
LS	40	147.4	285	9.8	11	38,130
MS	40	123.44	400	7.5	11.1	22,814
HS	42	50	390	5	11.1	8609

Table 7
Material price of different devices in three cases.

Device	Material	Price/$/t
Water wall	12Cr1MoVG	1143
Superheater	SA-213T91	1714
Reheater	SA-213T91	1714
Economizer	12Cr1MoVG	1143

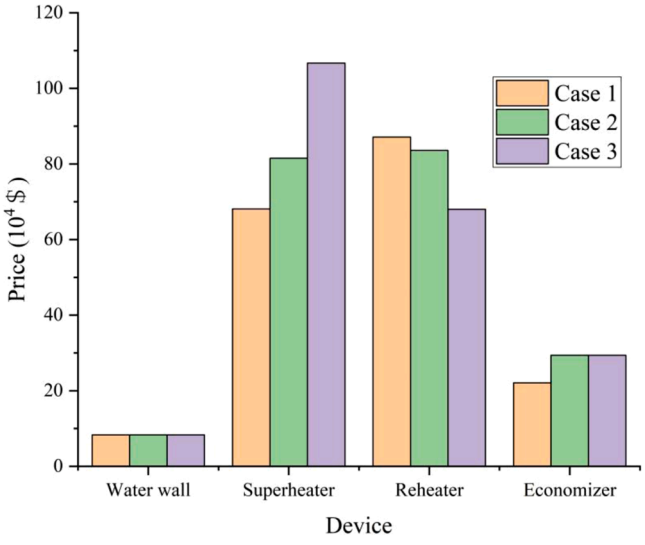

Fig. 9. Prices of different equipment under different cases for the new 600 MWe power plant.

power plant. While the heat exchange area in the cases 2 and 3 increases by about 47.3% and 53.7%, respectively.

(3) Pipe designs for the new 600 MWe coal-fired power plants under the three cases are similar. For case 1, the flue gas resistance of new coal-fired power plant is about 0.74 MPa.

(4) The economic analysis results indicate case 1 has a slight economic advantage compared with other cases, the price difference between the three cases is mainly reflected in the superheater and reheater of the new coal-fired power plant.

(5) The thermodynamic analysis results of new coal-fired power plant under three cases are consistent, and the system efficiency of new coal-fired power plant decreases as comparing to the benchmark coal-fired power plant.

This work is rarely involved in the current research progress, so this research provides the reference for the subsequent practical industrial application of coal-fired power plant coupled with CaO-based carbon capture system.

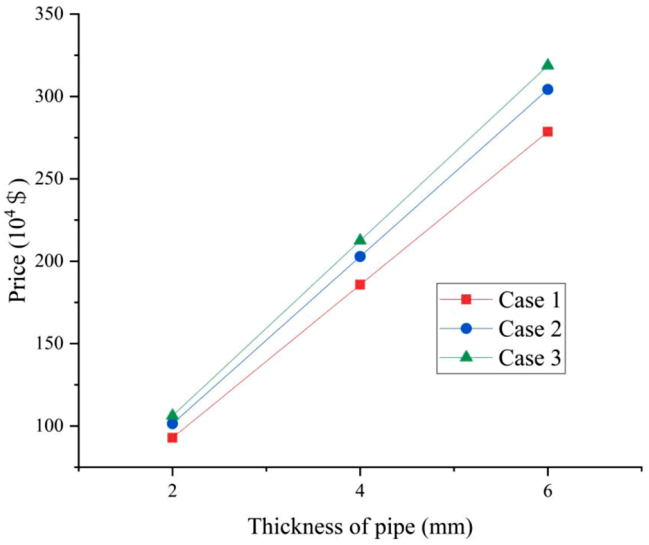

Fig. 10. Influence of pipe thickness on heating exchange device price of the new coal-fired power plant.

Table 8
Main results of three cases.

	Case 1	Case 2	Case 3	Benchmark coal-fired power plant
Heat exchange area/m^2	37,333	41,188	42,979	27,964
Feed water/t/h	1626.86	1627	1627	1612
Feed water scheme	In series	In parallel	In parallel	

CRediT authorship contribution statement

Zhixin Li: Conceptualization, Investigation, Software, Data curation, Writing – original draft. **Qinhui Wang:** Conceptualization, Writing – review & editing, Supervision, Funding acquisition. **Mengxiang Fang:** Supervision, Funding acquisition, Writing – review & editing. **Zhongyang Luo:** Supervision, Writing – review & editing.

Declaration of Competing Interest

The authors declare that they have no known competing financial interests or personal relationships that could have appeared to influence the work reported in this paper.

Acknowledgement

This work was supported by The National Key Research and Development Program of China (No. 2017YFB0603300).

References

[1] J. Bao, W.H. Lu, J. Zhao, X.T. Bi, Greenhouses for CO_2 sequestration from atmosphere, Carbon Resourc. Convers. 1 (2) (2018) 183–190, https://doi.org/10.1016/j.crcon.2018.08.002.
[2] T.M. Bachmann, Considering environmental costs of greenhouse gas emissions for setting a CO_2 tax: a review, Sci. Total Environ. 720 (2020), 137524, https://doi.org/10.1016/j.scitotenv.2020.137524.
[3] J. Liu, J. Baeyens, Y. Deng, T. Tan, H. Zhang, The chemical CO_2 capture by carbonation-decarbonation cycles, J. Environ. Manag. 260 (2020), 110054, https://doi.org/10.1016/j.jenvman.2019.110054.
[4] Y. Wu, X. Chen, J. Ma, Y. Wu, D. Liu, W. Xie, System integration optimization for coal-fired power plant with CO_2 capture by Na_2CO_3 dry sorbents, Energy 211 (2020), 118554, https://doi.org/10.1016/j.energy.2020.118554.
[5] F.A. Tobiesen, G. Haugen, A. Hartono, A systematic procedure for process energy evaluation for post combustion CO_2 capture: case study of two novel strong bicarbonate-forming solvents, Appl. Energy 211 (2018) 161–173, https://doi.org/10.1016/j.apenergy.2017.10.091.
[6] T. Shimizu, T. Hirama, H. Hosoda, K. Kitano, M. Inagaki, K. Tejima, A twin fluid-bed reactor for removal of CO_2 from combustion processes, Chem. Eng. Res. Des. 77 (1) (1999) 62–68, https://doi.org/10.1205/026387699525882.
[7] N. Rodriguez, M. Alonso, G. Grasa, J.C. Abanades, H.eat requirements in a calciner of $CaCO_3$ integrated in a CO_2 capture system using CaO, Chem. Eng. J. 138 (1–3) (2008) 148–154, https://doi.org/10.1016/j.cej.2007.06.005.
[8] M. Spinelli, I. Martínez, M.C. Romano, One-dimensional model of entrained-flow carbonator for CO_2 capture in cement kilns by Calcium looping process, Chem. Eng. Sci. 191 (2018) 100–114, https://doi.org/10.1016/j.ces.2018.06.051.
[9] P. Teixeira, I. Mohamed, A. Fernandes, J. Silva, F. Ribeiro, C.I.C. Pinheiro, Enhancement of sintering resistance of CaO-based sorbents using industrial waste resources for Ca-looping in the cement industry, Sep. Purif. Technol. 235 (2020), https://doi.org/10.1016/j.seppur.2019.116190.
[10] M. Bailera, P. Lisbona, L.M. Romeo, L.I. Díez, C.alcium looping as chemical energy storage in concentrated solar power plants: carbonator modelling and configuration assessment, Appl. Therm. Eng. 172 (2020), 115186, https://doi.org/10.1016/j.applthermaleng.2020.115186.
[11] R. Zhai, C. Li, J. Qi, Y. Yang, Thermodynamic analysis of CO_2 capture by calcium looping process driven by coal and concentrated solar power, Energy Convers. Manag. 117 (2016) 251–263, https://doi.org/10.1016/j.enconman.2016.03.022.
[12] X. Zhang, P. Song, L. Jiang, Performance evaluation of an integrated redesigned coal fired power plant with CO_2 capture by calcium looping process, Appl. Therm. Eng. 170 (2020), https://doi.org/10.1016/j.applthermaleng.2020.115027.
[13] L. Zhou, L. Duan, E.J. Anthony, A. calcium looping process for simultaneous CO_2 capture and peak shaving in a coal-fired power plant, Appl. Energy 235 (2019) 480–486, https://doi.org/10.1016/j.apenergy.2018.10.138.
[14] D.P. Hanak, C. Biliyok, E.J. Anthony, V. Manovic, Modelling and comparison of calcium looping and chemical solvent scrubbing retrofits for CO_2 capture from coal-fired power plant, Int. J. Greenh. Gas Control 42 (2015) 226–236, https://doi.org/10.1016/j.ijggc.2015.08.003.
[15] L. Duan, T. Feng, S. Jia, X. Yu, Study on the performance of coal-fired power plant integrated with Ca-looping CO_2 capture system with recarbonation process, Energy 115 (2016) 942–953, https://doi.org/10.1016/j.energy.2016.09.077.
[16] C. Ortiz, R. Chacartegui, J.M. Valverde, J.A. Becerra, A. new integration model of the calcium looping technology into coal fired power plants for CO_2 capture, Appl. Energy 169 (2016) 408–420, https://doi.org/10.1016/j.apenergy.2016.02.050.
[17] M. Romano, Coal-fired power plant with calcium oxide carbonation for postcombustion CO_2 capture, Energy Proced. 1 (1) (2009) 1099–1106, https://doi.org/10.1016/j.egypro.2009.01.145.
[18] M. Spinelli, I. Martínez, E. De Lena, G. Cinti, M. Hornberger, R. Spörl, M. C. Romano, I.ntegration of Ca-Looping Systems for CO_2 capture in cement plants, Energy Proced. 114 (2017) 6206–6214, https://doi.org/10.1016/j.egypro.2017.03.1758.
[19] W.S. Lee, J.H. Kang, J.C. Lee, C.H Lee, Enhancement of energy efficiency by exhaust gas recirculation with oxygen-rich combustion in a natural gas combined cycle with a carbon capture process, Energy 200 (2020), 117586, https://doi.org/10.1016/j.energy.2020.117586.
[20] D. Berstad, R. Anantharaman, K. Jordal, Post-combustion CO_2 capture from a natural gas combined cycle by CaO/$CaCO_3$ looping, Int. J. Greenh. Gas Control 11 (2012) 25–33, https://doi.org/10.1016/j.ijggc.2012.07.021.
[21] L.V. Pavão, J.A. Caballero, M.A.S.S. Ravagnani, C.B.B Costa, A pinch-based method for defining pressure manipulation routes in work and heat exchange networks, Renew. Sustain. Energy Rev. 131 (2020), 109989, https://doi.org/10.1016/j.rser.2020.109989.
[22] N. Jiang, W. Han, F. Guo, H. Yu, Y. Xu, N Mao, A novel heat exchanger network retrofit approach based on performance reassessment, Energy Convers. Manag. 177 (2018) 477–492, https://doi.org/10.1016/j.enconman.2018.10.001.
[23] B.H. Li, Y.E. Chota Castillo, C.T Chang, An improved design method for retrofitting industrial heat exchanger networks based on pinch analysis, Chem. Eng. Res. Des. 148 (2019) 260–270, https://doi.org/10.1016/j.cherd.2019.06.008.
[24] N.N. Ziyatdinov, I.I. Emel'yanov, Q. Chen, I.E. Grossmann, Optimal heat exchanger network synthesis by sequential splitting of process streams, Comput. Chem. Eng. 142 (2020), 107042, https://doi.org/10.1016/j.compchemeng.2020.107042.
[25] H.A. Kayange, G. Cui, Y. Xu, J. Li, Y Xiao, Non-structural model for heat exchanger network synthesis allowing for stream splitting, Energy 201 (2020), 117461, https://doi.org/10.1016/j.energy.2020.117461.
[26] L. Xia, Y. Feng, X. Sun, S Xiang, Design of heat exchanger network based on entransy theory, Chin. J. Chem. Eng. 26 (8) (2017) 1692–1699, https://doi.org/10.1016/j.cjche.2017.10.007.
[27] Y.Q. Lai, S.R. Wan Alwi, Z.A Manan, Graphical customisation of process and utility changes for heat exchanger network retrofit using individual stream temperature versus enthalpy plot, Energy 203 (2020), 117766, https://doi.org/10.1016/j.energy.2020.117766.
[28] Y. Wang, L. Cao, X. Li, J. Wang, P. Hu, B. Li, Y Li, A novel thermodynamic method and insight of heat transfer characteristics on economizer for supercritical thermal power plant, Energy 191 (2020), 116573, https://doi.org/10.1016/j.energy.2019.116573.
[29] F.N. Ridha, D.Y. Lu, R.T. Symonds, S. Champagne, Attrition of CaO-based pellets in a 0.1 MW_{th} dual fluidized bed pilot plant for post-combustion CO_2 capture, Powder Technol. 291 (2016) 60–65, https://doi.org/10.1016/j.powtec.2015.11.065.
[30] J. Hilz, M. Haaf, M. Helbig, N. Lindqvist, J. Ströhle, B. Epple, Scale-up of the carbonate looping process to a 20 MW_{th} pilot plant based on long-term pilot tests, Int. J. Greenh. Gas Control 88 (2019) 332–341, https://doi.org/10.1016/j.ijggc.2019.04.026.

[31] J. Ströhle, J. Hilz, B. Epple, Performance of the carbonator and calciner during long-term carbonate looping tests in a 1 MW_{th} pilot plant, J. Environ. Chem. Eng. 8 (1) (2020), 103578, https://doi.org/10.1016/j.jece.2019.103578.
[32] D. Wang, H. Li, C. Wang, Y. Zhou, X. Li, M Yang, Thermodynamic analysis of coal-fired power plant based on the feedwater heater drainage-air preheating system, Appl. Therm. Eng. 185 (2021), 116420, https://doi.org/10.1016/j.applthermaleng.2020.116420.
[33] J. Zhang, Z. Zhang, H. Fan, X. Ge, J. Dong, W Xu, Experimental study of heat transfer characteristics in a coal-fired test facility under advanced ultra-supercritical conditions, Fuel 267 (2020), 117255, https://doi.org/10.1016/j.fuel.2020.117255.
[34] Z. Li, Q. Wang, M. Fang, Z. Luo, Thermodynamic and economic analysis of a new 600 MWe coal-fired power plant integrated with CaO-based carbon capture system, Int. J. Greenh. Gas Control 109 (2021), 103386, https://doi.org/10.1016/j.ijggc.2021.